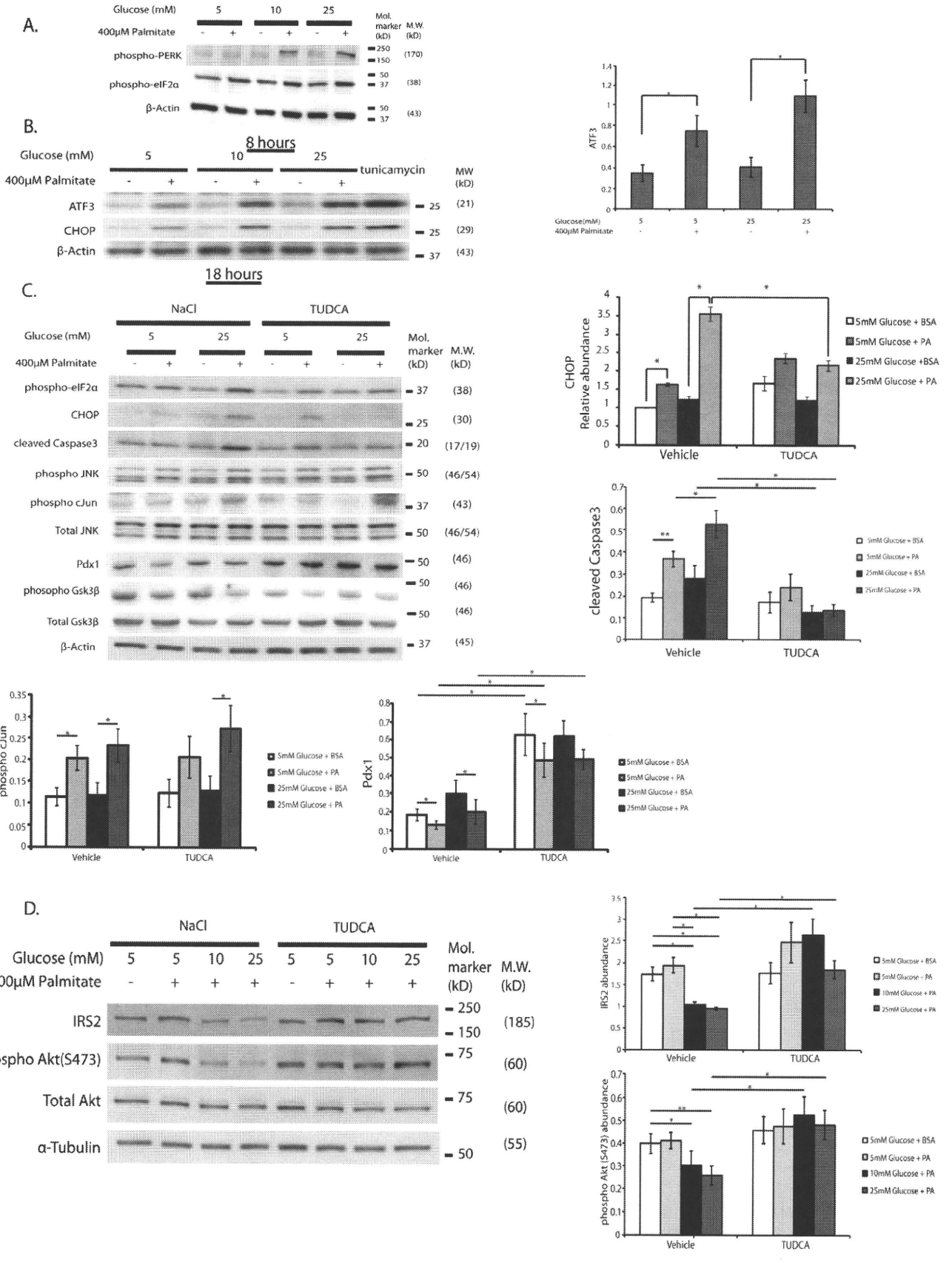


**Figure 3. The synergistic effects of glucose and palmitate on ER stress and reduction of insulin signaling is attenuated by addition of a chemical chaperon.** (**A**) MIN6 cells were treated with either control 0.5% BSA or 400 μM palmitate+0.5% BSA at a concentration of 5, 10, 25 mM glucose for 8 hours. Total cell lysates were extracted at indicated time points and were subjected to Western blot analysis using anti-

phospho-PERK (980Thr), anti-phopsho-eIF2α (51Ser), and (**B**) MIN6 cells were treated with either control 0.5% BSA or 400 μM palmitate+0.5% BSA at a concentration of 5, 10, 25 mM glucose for 18 hours and blotted with anti-ATF3 and anti-CHOP antibodies. β-Actin was detected for loading control. Tunicamycin treatment was control for ER stress. (**C**) Cells were treated with either 500 μg/ml NaCl (ionic control) or 500 μg/ml TUDCA 15-h prior to beginning of palmitate treatment and then were co-treated with either 0.5% BSA or 400 μM palmitate+0.5% BSA with either 5 mM or 25 mM glucose and NaCl or TUDCA for 24 h. Total cell lysates were subjected to Western blot analysis with antibodies to the indicated proteins. Densitometry of total CHOP and cleaved Caspase3 and Pdx1 were measured and normalized over α-Tubulin, respectively. Densitometry of phospho-cJun was measured and normalized over total JNK. The representative results of three individual experiments are shown. The effects on CHOP, cleaved Caspase3 and phospho-cJun and Pdx1 protein are graphically illustrated. *$p<0.05$. (**D**) Cells were treated with either 500 μg/ml NaCl (ionic control) or 500 μg/ml TUDCA 15-h prior to beginning of palmitate treatment and then were co-treated with either 0.5% BSA or 400 μM palmitate+0.5% BSA with either 5 mM, 10 mM or 25 mM glucose and NaCl or TUDCA for 24-h. Total cell lysates were subjected to Western blot analysis with antibodies to the indicated proteins. Densitometry of total IRS2 was measured and normalized over α-Tubulin and densitometry of phospho-Akt was measured and normalized over total Akt. The representative results of three individual experiments are shown. The effects on IRS2 protein are graphically illustrated, *$p<0.05$, **$p<0.01$.

doi:10.1371/journal.pone.0018146.g003

shRNA adenovirus constructs described previously [14] were incubated with the cells at an MOI of 30 for 4 hours in normal culture media. Palmitate and cytokine treatments were initiated 24 hours following removal of virus.

### Inhibition of Gsk3β expression with a kinase dead adenovirus

Adenovirus expressing a catalytic inactive mutant of the human Gsk3β (Adv-Gsk3βKM) was prepared as previously described [21]. Control adenovirus-green fluorescent protein (AdV-GFP) was a gift from D. Kelly (Washington University, St. Louis, MO). Infection of the MIN6 cells was carried out at the indicated multiplicity of infection (MOI) for one hour in serum-free media. The MIN6 were then washed in PBS, maintained in the DMEM/15% FBS media, and then experiments were carried out 24 hours after infection.

### Statistical analysis

The presented data were analyzed from at least 3 independent experiments and are shown as means ±S.E.M. The significance of the variations was analyzed using either a one- or two-way ANOVA with Bonferroni corrections with a significance level of 0.05 (95% confidence intervals).

## Results

### Glucose and palmitate synergize to induce apoptosis

Our previous study had shown a dose-dependent effect of FFA, both palmitate (50–400 μM) and oleate (50–400 μM), on ER stress and apoptosis in glucose-responsive insulinoma (MIN6) cells [16]. In the current study the dose-dependent effect of glucose (5–25 mM) was examined at 400 μM palmitate. As shown in Figure 1A, increasing glucose concentration had a clear synergistic effect on cell death characterized by propidium iodide incorporation normalized to DAPI staining. While 400 μM palmitate resulted in about 3% propidium iodide incorporation at 5 mM glucose, this was increased more than threefold when the glucose concentration was raised to 15 mM and 25 mM. While there was no effect of palmitate on cleaved Caspase3 at 5 mM glucose, consistent with the synergism observed on propidium iodide staining, glucose and palmitate also synergized on activation of the pro-apoptotic marker cleaved Caspase3 comparing that at 5 mM glucose/palmitate vs. 25 mM glucose/palmitate, $p<0.05$ (Figure 1B).

We next explored the underlying mechanisms for the glucose potentiation. FFA treatment has been shown to induce JNK activation that can contribute to FFA-induced apoptosis; we determined the effects of altering glucose concentrations on JNK activation. Interestingly, JNK activation by FFA was maximal at the lowest glucose concentration and did not increase further as glucose was increased (Figure 1B). Maximal FFA activation of JNK at 5 mM glucose with apparent increasing activation of cleaved Caspase3 with increasing glucose concentration suggested that further enhancement of JNK by glucose could not explain the synergistic effects on cell death.

### Glucose and palmitate synergize to reduce insulin signaling associated with a decrease in IRS2 protein

Previous studies have shown that glucose treatment of insulinoma cells results in activation of the insulin receptor substrate-PI3-kinase-Akt pathway that serves to protect against β-cell death. In contrast, FFA treatment of insulinoma cells inhibits this pathway [8,16]. We examined whether the synergistic effect of glucose on FFA-induced apoptosis could be related to inhibition of this signaling pathway. Glucose alone (5–25 mM), as shown in the first four lanes of Figure 2, increased phospho-Akt (S473) and phospho-Gsk3 as expected, with no apparent change in IRS1 or IRS2 proteins, confirming previous observations [8,22]. However as glucose was raised in the presence of palmitate (Figure 2, lanes 5–8) a dose-dependent decrease in phospho-Akt and phospho-Gsk3β were observed and accompanied by a parallel decrease in IRS2, while IRS1 levels did not appear to change. This synergistic effect of increasing glucose in the presence of FFA on inhibition of IRS2 and PI-3 kinase-Akt signaling is a novel finding that might explain the synergistic effect on β-cell survival [23].

### The effect of glucose and FFA is accompanied by a synergistic effect on ER stress that is reduced by addition of a chemical chaperone

FFA impair insulin signaling in β-cells in part via activation of ER stress [16,24]. Bachar et. al. [13] recently showed in insulinoma cells that palmitate at 22.2 mM glucose vs. 3.3 mM glucose increased activation of JNK, CHOP and the ER stress enzyme phospho-PERK. We examined the effects of increasing glucose from 5 mM to 25 mM at 8 and 18 hours of treatment to observe the different time course of development of ER stress markers. An enhancement of the ER stress markers phospho-PERK, phospho-eIF2α, CHOP, and ATF3 (Figure 3A and 3B) was observed, confirming and extending the results of Bachar et. al. [13]. The observation that glucose appeared to synergize with palmitate to increase ATF3 protein expression, although this was not statistically significant, was consistent with the previous finding by Hartman et. al. demonstrating that high glucose and FFA together increased ATF3 mRNA expression, and that this was associated with increased apoptosis of insulinoma cells [25]. These glucose-induced changes in the presence of palmitate on ER stress markers were again noted in the absence of phospho-c-Jun (Figure 3C).

We next examined whether reducing ER stress using TUDCA, a chemical chaperone that enhances ER functional capacity [26],

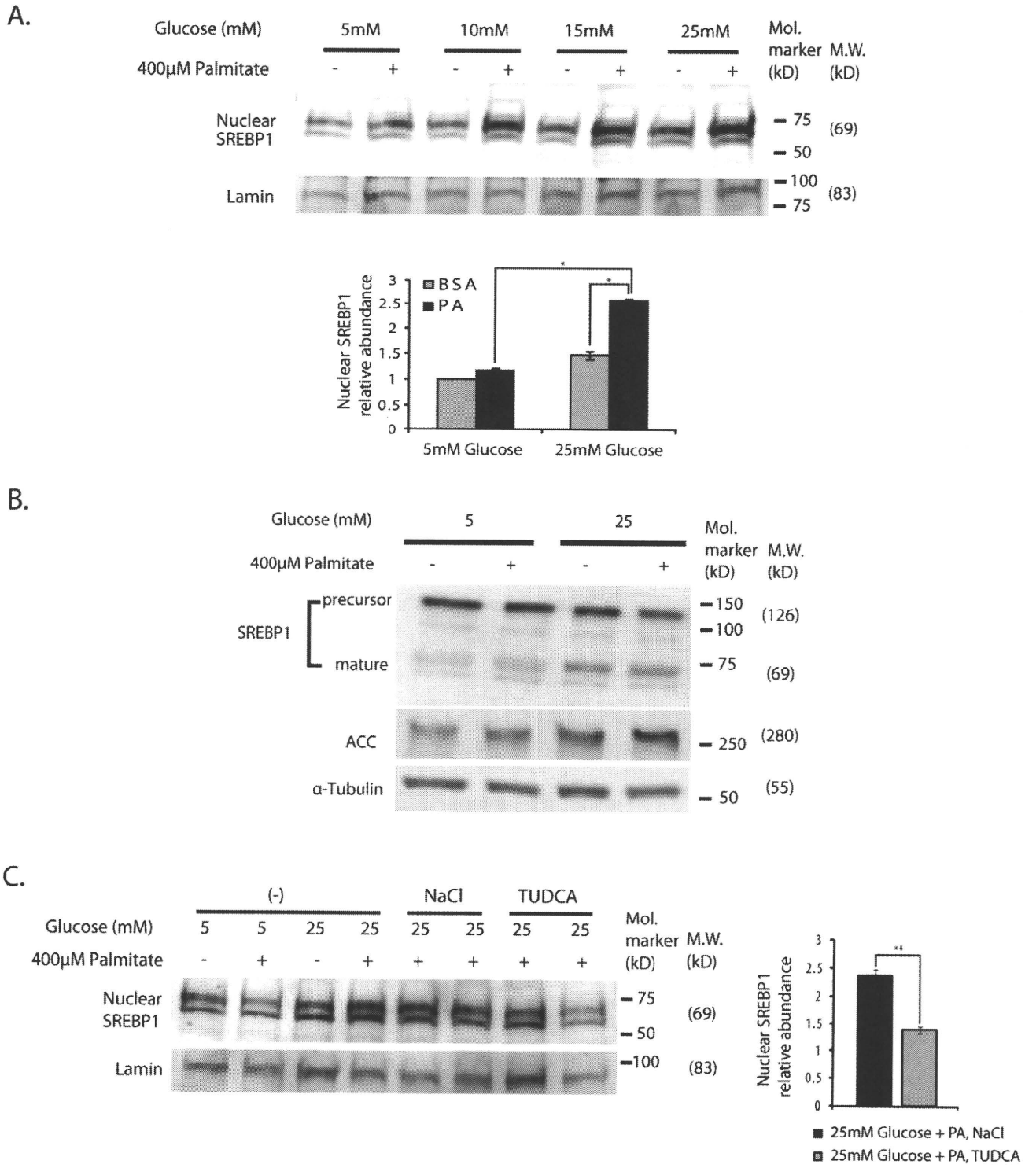


**Figure 4. The synergistic effects of glucose and palmitate on ER stress results in concomitant effects on activation of SREBP1.** (**A**) MIN6 cells were treated with either control 0.5% BSA or 400 μM palmitate+0.5% BSA at a concentration of 5, 10, 15, 25 mM glucose for 18-h. Nuclear fractions were extracted from the cells and were subjected to Western blot analyses using anti-SREBP1 and anti-Lamin antibodies. 25 μg of nuclear protein was loaded in each lane. The upper band normalized over Lamin was used to do the quantification (the lower band is nonspecific). The relative ratio of nuclear SREBP1 over Lamin calculated by densitometries was summarized as means ± S.E.M. in the graph respectively. The representative results of three experiments are shown, and graphically illustrated, * $p<0.05$. (**B**) MIN6 cells were treated with either control 0.5% BSA or 400 μM palmitate+0.5% BSA at a concentration of either 5 or 25 mM glucose for 24-h. Total cell lysates were subjected to Western blot analysis using anti-acetyl CoA carboxylase (ACC) and anti-α-Tubulin antibodies. The representative results of two individual experiments are shown. (**C**) Cells were treated with either 500 μg/ml NaCl or 500 μg/ml TUDCA 15-h prior to beginning of palmitate treatment. Cells were co-treated with either 0.5% BSA or 400 μM palmitate+0.5% BSA with 25 mM glucose and NaCl or TUDCA for 18-h. Nuclear fractions were extracted from the cells and were subjected to Western blot analyses using anti-SREBP1 and anti-Lamin antibodies. The upper band normalized over Lamin was used to do the quantification (the lower band is nonspecific). 25 μg of nuclear extracts were loaded in each lane. The representative results of three individual

experiments are shown. The relative ratio of nuclear SREBP1 over Lamin calculated by densitometries was summarized as means ± S.E.M. in the graph respectively **p<0.01.
doi:10.1371/journal.pone.0018146.g004

can reverse the synergistic effects of glucose and FFA on insulin receptor substrate signaling. As shown in Figure 3C, the effects of 24 hour treatment with 5 mM or 25 mM glucose in the presence and absence of palmitate (400 μM) on activation of JNK and other markers of ER stress are shown in the control condition with NaCl (first 4 lanes). The results of protein expression under the same conditions but in the presence of TUDCA are shown in the last 4 lanes of Figure 3C. JNK activation, which again was not augmented by the combination of high glucose and palmitate, was little affected by TUDCA treatment. In contrast the other ER stress markers phospho-eIF2α, CHOP and cleaved Caspase 3 were attenuated by co-treatment with TUDCA. Addition of TUDCA also increased Pdx1 (Figure 3C). The increase in phospho-Akt protein levels, an inhibitor of Gsk3 activity, and IRS2 protein levels were also observed with TUDCA treatment (Figure 3D). Together the results suggest that glucose potentiation of FFA induced apoptosis involves activation of ER stress with resultant inhibition of insulin signaling in a manner independent of further JNK activation.

## Glucose and palmitate synergistically activate SREBP1

Sterol regulatory element-binding protein-1 (SREBP1) is a transcription factor that stimulates expression of lipid-regulatory genes [27]. SREBP1 is an ER membrane resident protein that in response to sterol depletion is cleaved to generate a transcriptionally active N-terminal fragment that translocates to the nucleus [28]. SREBP1 is increased in liver and islets of diabetic animals [29]. *In vivo* SREBP1 overexpression increased lipid accumulation in islets, reduced β-cell mass, and impaired insulin secretion [30]. Overexpression of the SREBP1 gene in insulinoma and islet β-cells also reduced IRS2 protein [31]. Furthermore, incubation of insulinoma cells and islets with high glucose (25 mM) was shown to activate SREBP1. The latter study examined only high glucose, and did not include FFA. As shown in Figure 4A, like the study of Wang et. al [31] we observed an apparent slight effect of increasing glucose on SREBP1 activation, when nuclear SREBP1 was corrected for nuclear Lamin. A synergistic effect was observed of glucose and FFA on activation of SREBP1 with a concomitant reduction of SREBP1 precursor and appearance of mature or nuclear SREBP1. SREBP1 activation was further confirmed by increased expression of its target acetyl-CoA carboxylase (ACC) (Figure 4B). SREBP1 activation was reduced by attenuation of ER stress with TUDCA pretreatment (Figure 4C) that suggested that the synergistic effects of glucose and palmitate on activation of SREBP1 were mediated by exacerbation of ER stress.

## Glucose/palmitate activate ER stress and reduce insulin signaling in primary islets

To validate the relevance of synergistic effects of glucose and palmitate on pancreatic β-cells we treated isolated primary mouse islets with 11 mM or 30 mM glucose in either the absence or presence of 400 μM palmitate for 72 hours. This incubation time and different glucose concentrations were utilized as it was determined that primary islets are more resistant to FFA induced apoptosis than are insulinoma cells (data not shown). Treatment with high glucose (30 mM) and palmitate resulted in an apparent but not significant ($p = 0.14$) enhanced induction of cleaved Caspase3 (Figure 5A), and an apparent but not significant ($p = 0.07$) reduced IRS2 expression (Figure 5B). In addition, high glucose and palmitate synergistically enhanced the ER stress marker GRP78 ($p<0.05$) beyond JNK activation (Figure 5C), and caused an apparent increase in ATF3 ($p = 0.06$) (Figure 5D). Consistent parallel increases in nuclear SREBP1 and total ACC protein also appeared to be potentiated by high glucose and palmitate although the effects were not significant (Figure 5E). Treatment with high glucose and palmitate did however result in significant reduction of phospho-Akt, Pdx1, and phospho-Gsk3b with no change in phospho-cJun (Figure 5F). These data together support the relevance of findings in insulinoma cells to primary islet β-cells.

## Loss-of-function of ATF3 and gain-of function of IRS2 reduce the effects of glucose and palmitate on apoptosis

To assess the effects of ER stress-induced ATF3 expression and subsequent suppression of IRS2 on glucolipotoxicity mediated apoptosis, loss- and gain-of-function studies were conducted. INS-r3 cells were utilized as the reagents for small hairpin RNA (shATF3) were controlled for rat ATF3 and not mouse. A similar role for ATF3 in MIN6 and INS1 insulinoma cell stress response has been observed (Zmuda and Hai, unpublished observations). INS-r3 cells were incubated with 400 μM palmitate/25 mM glucose for the indicated times in the presence of adenoviruses expressing either control or shATF3 to reduce ATF3 expression [14]. Note that phospho-Akt appeared to be elevated in cells expressing shATF3 at all times consistent with the known inhibitory effect of ATF3 on IRS2 transcription and subsequent insulin signaling. The IRS2 levels in the ATF3 knockdown cells appeared to be elevated relative to that in control cells at both 8 and 16 hours of glucose/palmitate treatment. Further cleaved Caspase3, following glucose/palmitate treatment, was suppressed in ATF3 knockdown cells ($p<0.002$). The conclusion that ER stress activates ATF3 that contributes to impaired insulin signaling and apoptosis is thus supported by these ATF3 knockdown experiments.

In another experiment using primary islets treated with glucose/palmitate for 72 hours, the effects of transfection with an adenovirus expressing IRS2 was compared to that of islets with control adenovirus. As shown in Figure 6B, where Immunodetection was set to assess high levels of IRS2 in IRS2 transfected cells, there was a marked increase in IRS2 protein with IRS2 overexpression. Glucose/palmitate treatment resulted in increased ATF3 and cleaved Caspase3 with control adenovirus, while overexpression of IRS2 appeared to reduce the degree of apoptosis as measured by reduction of cleaved Caspase3 (Figure 6B). These results are consistent with the previously demonstrated role of ATF3 on ER stress induced apoptosis in islets [14,25].

## Loss-of-function of Gsk3β on glucose and palmitate induced β-cell apoptosis

The progressive decline in insulin receptor substrate signaling observed with decreasing IRS2 expression and phospho-Akt was associated with decreased phosphorylation of Gsk3β (Figure 2) and thus activation of the pro-apoptotic form of Gsk3β [32]. To examine the contribution of activation of Gsk3β, the effects of palmitate treatment with increasing amounts of an adenovirus expressing a catalytic inactive mutant of the human Gsk3β (Adv-Gsk-3βKM) were analyzed by Western blot (Figure 7A). A control sample was placed on either end of the blot to facilitate

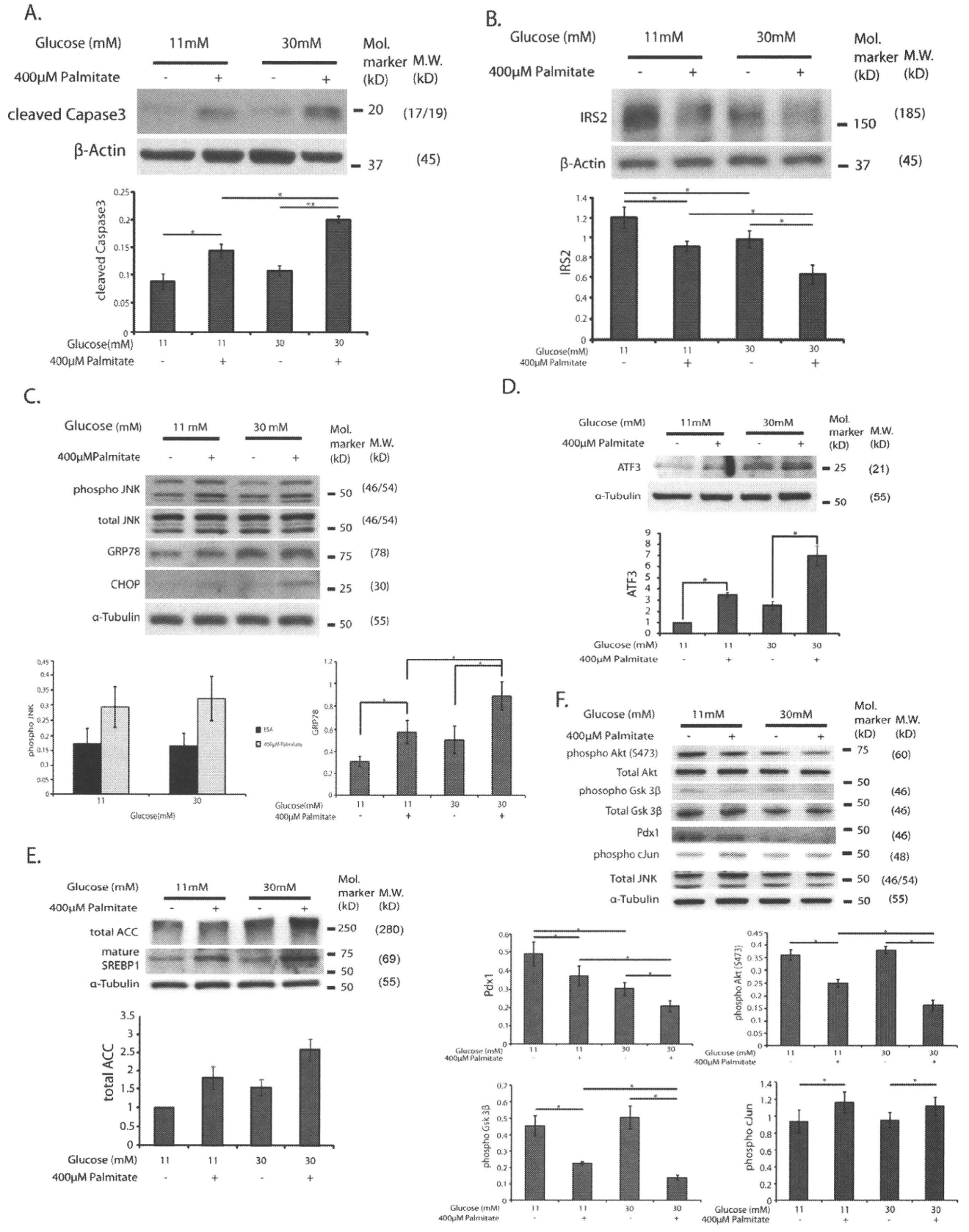


**Figure 5. Synergistic effects of glucose and palmitate on ER stress and suppression of IRS2 expression levels in primary mouse islets.** Islets from 14 weeks of age C57BL/6 male mice were isolated as described in Methods and were treated with either control 0.5% BSA or 400 μM palmitate+0.5% BSA in RPMI medium containing either 11 mM or 30 mM glucose, 10% FBS for 72-h. Total cell lysates were extracted from

the islets and subjected to Western blot analysis using (**A**) anti-cleaved Caspase3 and anti-β-Actin, (**B**) anti-IRS2 antibodies, (**C**) anti-phospho-JNK, anti-total JNK, anti-GRP78, anti-CHOP, anti-α-Tubulin antibodies, (**D**) anti-ATF3 antibodies, (**E**) anti-Acetyl CoA Carboxylase (ACC), anti-SREBP1, anti-α-Tubulin antibodies, (**F**) anti-Pdx1, anti-phospho-Gsk3β, anti-total Gsk3β, anti-phospho-Akt (S473), anti-phospho-cJun, anti-α-Tubulin antibodies. The blots shown are representative of 3 individual islet experiments. The relative ratio of indicated protein over β-Actin or α-Tubulin as a loading control calculated by densitometries was summarized as means ± S.E.M. in the graph respectively *$p<0.05$, **$p<0.01$.
doi:10.1371/journal.pone.0018146.g005

comparisons. For instance, observe the increase in cleaved Caspase3 and phopho-JNK between the two controls on either end of the blot. Increasing doses of the virus correlated with increased levels of total Gsk-3β, and reduced levels of the Gsk-3β substrate phospho-GS. Increased kinase dead Gsk-3β virus also resulted in increased expression of Pdx1, reduced apoptosis as suggested by cleaved Caspase 3 levels, and cell death measured by propidium iodide incorporation (Figure 7B). Interestingly the protective effects of the Adv-Gsk-3βKM occurred in spite of apparent comparable activation of phospho-JNK with palmitate treatment.

## Discussion

The combination of hyperglycemia and hyperlipidemia that is associated with insulin resistance may contribute to reducing β-cell mass and promoting the transition to full blown Type 2 diabetes, but the underlying mechanisms are only partially understood. This study examined the sequence of molecular events that may be involved in this process, and resulted in several novel observations: 1) While early induction of JNK plays a role in FFA-induced apoptosis [13,16], it does not appear involved in the high glucose potentiation of FFA effects; 2) the potentiating effects of glucose and FFA on ER stress result in activation of ER-associated SREBP1 and ATF3 leading to reduced IRS2 expression further impairing insulin-receptor substrate-PI-3K-Akt signaling, and 3) treatment with an adenovirus expressing a kinase dead Gsk3β significantly restored Pdx1 levels, and reduced the apoptosis induced by high glucose and FFA. Together these findings provide a molecular model for the synergistic effects of glucose and FFA on islet cell death and identify potentially useful therapeutic targets.

The role of JNK activation in FFA-induction of apoptosis in β-cells has been documented [13,16,33]. In the current study, JNK activation by palmitate was significant as expected, but was maximal at low glucose, and glucose potentiation of FFA-induced apoptosis was JNK independent (Figure 1B). How FFA treatment of β-cells leads to JNK activation is not completely known, but FFA induce ER stress, which activates JNK activation, and JNK activation itself can induce ER stress [13,34]. Interestingly, TUDCA appeared to reduce cleaved Caspase3 and CHOP induction, while not appearing to reduce JNK activation (Figure 3) suggesting that in this case JNK activation is upstream of ER stress. On the other hand the results of inhibition of ATF3 by shRNA in Figure 6A suggest that JNK activation is upstream of ER stress. Our results do not therefore settle this issue of the relative position of JNK activation and ER stress. Regardless of whether JNK activation is upstream or downstream of ER stress, the findings in the current study show that the combination of high glucose and FFA does not associate with further activation of JNK as compared to FFA in low glucose. This result is to some extent in conflict with that of Bachar et. al. [13] who showed that incubating islet cells in low vs. high glucose resulted in both increased ER stress and JNK activation. A difference in the two experiments is that Bachar et.al. evaluated islet cells in 3.3 mM vs. 22 mM glucose, and our experiments assessed cells in 5.5 mM vs. 25 mM glucose. Our results do not rule out the contributory effect of JNK on β-cell apoptosis as previously shown [13,16,33] but they emphasize the importance of additional mechanisms contributed by high glucose. Additionally, since glucose and palmitate have been shown to evoke oxidative stress, impairing nuclear translocation of Pdx1 and triggering β-cell failure [35], it is conceivable that oxidative stress interacts with JNK, ATF3 and ER stress to contribute to glucose/palmitate induced apoptosis, although this hypothesis remains to be tested.

The role of SREBP1 in high glucose induced apoptosis in islet β-cells has been reported [31]. In the absence of FFA, high glucose alone for 48 hours was shown to activate SREBP1 and to repress IRS2 and Pdx1 levels. Expression of a dominant negative SREBP1 reversed these transcriptional effects. In the current study, glucose alone at high concentration slightly activated SREBP1 as shown in Figure 4, an event that did not correlate with ER stress or apoptosis. A much more significant activation of SREBP1 was observed with glucose and palmitate together and this was shown to be a function of induced ER stress since it was attenuated by TUDCA (Figure 4C). These results only show an association of SREBP1 nuclear translocation, and do not document its causal role. It is likely however that SREBP1 nuclear translocation participates in glucose/palmitate induced apoptosis, as previous studies documented the causal role of SREBP1 in ER stress induced apoptosis in insulinoma cells [31]. SREBP1 resides in the ER membrane, where it is anchored by the labile protein INSIG1 [36]. The link between ER stress and SREBP1 activation has been little studied. Lee et. al. using CHO cells [36] showed that thapsigargin, a chemical that induces ER stress, activates SREBP1 due to rapid degradation of INSIG1 [36]. We observed that glucose and palmitate together appeared to reduce INSIG1 protein (data not shown), which likely contributed to augmentation of nuclear SREBP1 under these conditions.

Similarly a synergistic effect of glucose and FFA was observed on expression of the ER-associated stress marker ATF3. ATF3 expression paralleled suppression of IRS2 protein levels, and induction of apoptosis measured by CHOP (Figure 3A–B), and Caspase3 activation (Figure 3A). The association of ATF3 with ER stress and cell death has been well documented [37] but there is relatively little known related to ATF3 targets [14]. Recently, ATF3 was shown to suppress the IRS2 protein by binding to the IRS2 promoter [14] and implicated this mechanism in apoptosis induced by agents such as γ-interferon, TNF-α, or thapsigargin. Our findings are consistent with the involvement of ATF3 in the apoptotic effects of nutrient induced ER stress in islet cells. In this context, we note that Cunha et. al. [33] did not find a pro-apoptotic role of ATF3 in the context of palmitate treatment. Potential explanations for this apparent difference include the difference in glucose concentration (25 mM glucose in our study and 11 mM glucose in theirs), the cells used (INS-r3 in our study and INS-1E in theirs), and assays (activated Caspase3 in our study and propidium iodide plus Hoechst stain). An interesting question is whether ATF3 is a direct repressor of Pdx1 expression. Insulin signaling alters Gsk3β and FoxO activity [16,32,38,39] and these proteins are known regulators of Pdx1 expression. As ATF3 represses IRS2 and insulin signaling, at least part of ER stress and ATF3 induced Pdx1 suppression is due to decreased insulin signaling, and perhaps also due to direct suppression of Pdx1 expression, but this latter question remains to be determined by future experiments. Interestingly

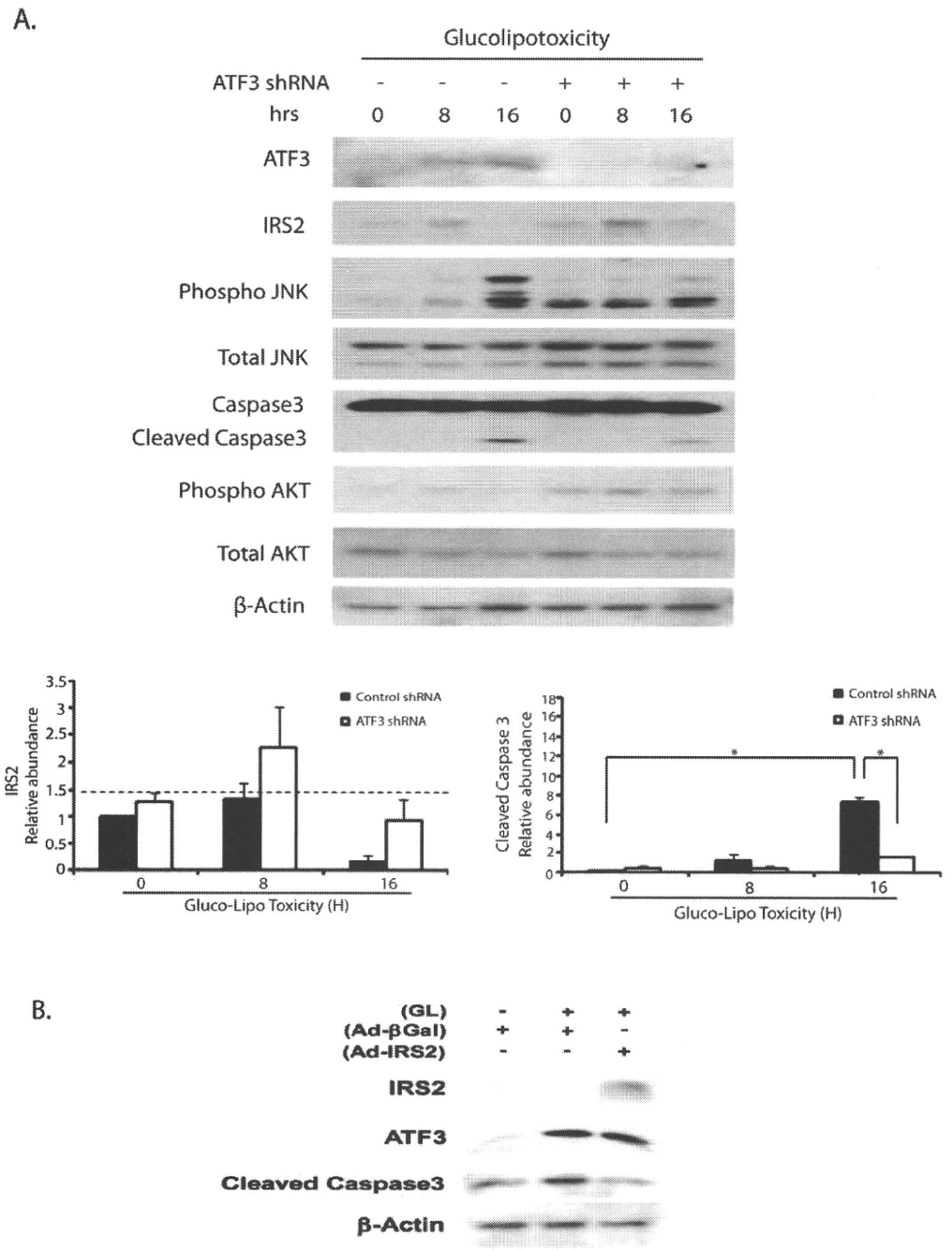


**Figure 6. Loss-of-function of ATF3 and gain-of function of IRS2 reduce the effects of glucose and palmitate on apoptosis.** (**A**) INS-r3 cells were infected with either control or ATF3 shRNA adenovirus 24-h prior to treatment with 400 μM palmitate+0.5% BSA and 25 mM glucose for the indicated times. Total cell lysates were obtained and subjected to Western blot analysis with antibodies to the indicated proteins. The relative ratio of IRS2 and cleaved Caspase3 expression over β-Actin was quantified by densitometry. The data obtained from three individual experiments are expressed as means ± S.E.M. * $p<0.02$, ** $p<0.012$. (**B**) In a single experiment, primary mouse islets were infected with adenovirus expressing βgal or IRS2 expressing adenovirus prior to treatment with either control 0.5% BSA and 5.5 mM glucose or 400 μM palmitate+0.5% BSA and 25 mM glucose for 72-h. "GL" refers to incubation in 25 mM glucose and 400 μM palmitate. Total cell lysates were subjected to Western blot using antibodies to indicated proteins.
doi:10.1371/journal.pone.0018146.g006

ATF3 induction is dependent on the P38 kinase pathway [15] which is part of signaling transduced by the membrane fatty acid translocase CD36 and a role of CD36, which is induced by glucose, has been proposed in mediating palmitate induced apoptosis of kidney tubular epithelial cell [40]. The role of this pathway in islet cells will need to be explored in future studies.

In the current studies we have shown a correlation among suppression of IRS2 protein levels (Figure 2), ATF3 expression (Figure 3), and resultant induction of apoptosis. The causal relationships among these events were demonstrated by Li. et. al. [14] when insulinoma cells and/or mouse islets were transfected with adenoviruses expressing inducible gain- or loss-of-function of ATF3

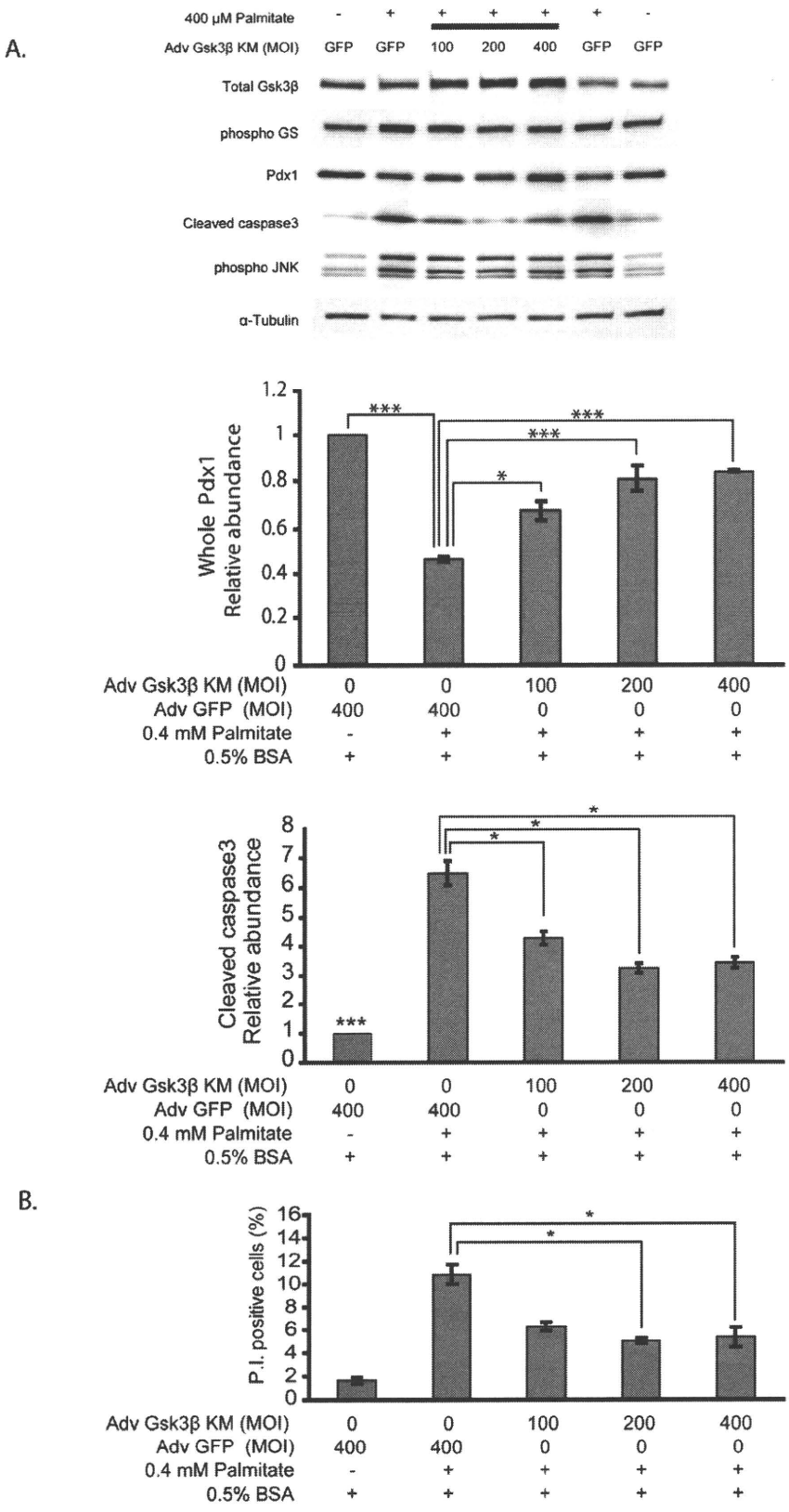


**Figure 7. Inhibition of Gsk3β protects against glucose and palmitate-induced apoptosis in MIN6 cells.** MIN6 cells were infected with 100, 200, or 400 MOI of adenovirus expressing a catalytically inactive mutant of the human Gsk3β (Adv-Gsk3βKM) or adenovirus expressing GFP (Adv-GFP) 24 hours prior to palmitate treatment. Cells were treated with 25 mM glucose and with either 0.5% BSA or 400 μM PA+0.5% BSA for 24 hours. A GFP control was placed on either end of the blot to facilitate comparison of control and Adv-Gsk3βKM. (**A**) Western blots using the indicated antibodies, with relative expression of Pdx1 normalized over α-Tubulin, and expression levels of cleaved Caspase3 normalized over α-tubulin. (**B**) Percentage of Propidium Iodide incorporation (n = 3, means ± S.E.M., *p<0.05, *** p<0.001).
doi:10.1371/journal.pone.0018146.g007

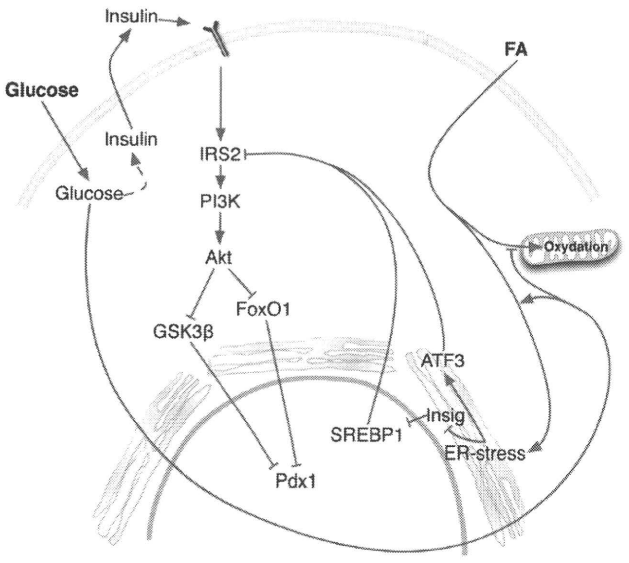


**Figure 8. Working diagram illustrating some of the key steps involved in "glucolipotoxicity" of β-cells.** High glucose and FFA together result in a vicious negative cycle that ultimately promotes β-cell death. As suggested by our findings, high glucose addition to FFA treated β-cells results in much more activation of SREBP1 than glucose alone. SREBP1 enhances ACC expression with generation of malonyl-CoA which impairs FFA oxidation. This in turn leads to augmented ER stress with further activation of ER-localized SREBP1 as a result of degradation of the anchoring protein Insig1. The excess non-metabolized FFA due to more impairment of FFA oxidation would partition in ER membranes compounding ER stress. In addition to SREBP1, ER stress activates ATF3. Both nuclear SREBP1 and ATF3 result in inhibition of IRS2, with concomitant impairment of insulin signaling, activation of Gsk3β and reduction of Pdx1 leading to apoptosis.
doi:10.1371/journal.pone.0018146.g008

and IRS2. Treatments that induced ATF3 activation and IRS2 suppression included induction of apoptosis by combined treatment of insulinoma cells with γ-interferon, TNF-α, or the ER stress activator thapsigargin. These studies demonstrated that ATF3, like the transcription factor CREB, alters IRS2 expression by binding to the IRS2 promoter. In the current study, we have examined the role of combined glucose and palmitate on this pathway (Figure 6). Transduction with an adenovirus expressing shATF3 significantly reduced this effect, while transduction with AdV-IRS2 ameliorated the apoptotic effect, thus mechanistically linking this pathway.

In this study co-incubation of insulinoma cells with an adenovirus expressing a kinase dead Gsk3β (Adv-Gsk3βKM, Figure 7) along with high glucose and palmitate for 24 hours significantly reduced cleaved Caspase3 and cell death. A previous study in IRS2 null mice had demonstrated that the severe diabetes associated with markedly increased apoptosis and reduced proliferation of islet β-cells was reversed when crossed with Gsk3β haploinsufficient mice [32]. The double knockout was also associated with enhanced expression of Pdx1 in islet β-cells. Like the IRS2 null mice with severe insulin resistance, glucose and FFA treatment of insulinoma cells and primary islets induces a state of insulin resistance. Also like IRS2 null mice on the Gsk3β genetic deficient background, reducing Gsk3β activity with a kinase dead Gsk3β adenovirus restored Pdx1 levels and reduced apoptosis and cell death. These findings emphasize the contribution of impaired insulin receptor substrate signaling in the apoptosis of β-cells treated with glucose and FFA, and the contribution of Gsk3β activity to this process.

A schematic diagram highlights the key concepts implied by our findings (Figure 8). In the insulin resistant subject abnormal metabolism of FFA and glucose result in chronically high levels of both nutrients in the circulation [41]. Under such conditions, the combination of hyperglycemia and FFA has been suggested to be particularly harmful for β-cells leading to so-called glucolipotoxicity [6,42,43]. Our findings suggest that addition of high glucose to FFA treated β-cells results in an escalating negative cycle. Under such conditions activation of the transcription factor SREBP1 leads to enhanced ACC expression with generation of malonyl-CoA (MCC), which impairs FFA oxidation. These in turn lead to ER stress with further activation of SREBP1, ATF3, and impairment of FFA oxidation. The excess unmetabolized FFA would partition in ER membranes compounding ER stress. Additionally nuclear SREBP1 and ATF3 result in inhibition of IRS2, with concomitant impairment of insulin receptor substrate signaling, increase of Gsk3β activity and reduction of Pdx1 leading to apoptosis. Several steps in the cycle shown in Figure 8 may be amenable to therapeutic intervention. These include the impairment of FFA oxidation by glucose, the synergistic effects of glucose and FFA on ER stress, the activation of SREBP1 and its negative effects on insulin signaling, and the downstream mediators of apoptosis that are activated by reduced IRS-signaling involving both Gsk-3β and Fox01.

The results of the current studies illustrate some of the potential mechanisms whereby a combination of high glucose and FFA, as occurs in insulin resistant subjects, may result in eventual destruction of β-cells. However, the ultimate contribution of these mechanisms to the etiology of β-cell failure and diabetes remains unknown and will need to be validated *in vivo*.

## Author Contributions

Conceived and designed the experiments: MAP YT YL SCM CCM EBM EZ TH NAA. Performed the experiments: KT YL CMW EZ. Analyzed the data: KT YL SDH SCM CCM EBM YT CJR EZ TH NAA MAP. Contributed reagents/materials/analysis tools: SCM CMW CJR EZ. Wrote the paper: KT YL SDH CCM EBM YT TH NAA MAP.

## References

1. Butler AE, Janson J, Bonner-Weir S, Ritzel R, Rizza RA, et al. (2003) Beta-cell deficit and increased beta-cell apoptosis in humans with type 2 diabetes. Diabetes 52: 102–110.
2. Weir GC, Laybutt DR, Kaneto H, Bonner-Weir S, Sharma A (2001) Beta-cell adaptation and decompensation during the progression of diabetes. Diabetes 50 Suppl 1: S154–159.
3. Unger RH (2001) [Maurice Derot Prize 2001. The liporegulator system and disease]. Journ Annu Diabetol Hotel Dieu. pp 129–143.
4. Donath MY, Halban PA (2004) Decreased beta-cell mass in diabetes: significance, mechanisms and therapeutic implications. Diabetologia 47: 581–589.
5. Zhou YP, Grill VE (1994) Long-term exposure of rat pancreatic islets to fatty acids inhibits glucose-induced insulin secretion and biosynthesis through a glucose fatty acid cycle. J Clin Invest 93: 870–876.
6. Poitout V, Robertson RP (2008) Glucolipotoxicity: fuel excess and beta-cell dysfunction. Endocr Rev 29: 351–366.
7. Cnop M (2008) Fatty acids and glucolipotoxicity in the pathogenesis of Type 2 diabetes. Biochem Soc Trans 36: 348–352.
8. Wrede CE, Dickson LM, Lingohr MK, Briaud I, Rhodes CJ (2002) Protein kinase B/Akt prevents fatty acid-induced apoptosis in pancreatic beta-cells (INS-1). J Biol Chem 277: 49676–49684.
9. Kharroubi I, Ladriere L, Cardozo AK, Dogusan Z, Cnop M, et al. (2004) Free fatty acids and cytokines induce pancreatic beta-cell apoptosis by different mechanisms: role of nuclear factor-kappaB and endoplasmic reticulum stress. Endocrinology 145: 5087–5096.
10. Cnop M, Ladriere L, Hekerman P, Ortis F, Cardozo AK, et al. (2007) Selective inhibition of eukaryotic translation initiation factor 2 alpha dephosphorylation potentiates fatty acid-induced endoplasmic reticulum stress and causes pancreatic beta-cell dysfunction and apoptosis. J Biol Chem 282: 3989–3997.
11. Pirot P, Ortis F, Cnop M, Ma Y, Hendershot LM, et al. (2007) Transcriptional regulation of the endoplasmic reticulum stress gene chop in pancreatic insulin-producing cells. Diabetes 56: 1069–1077.

12. Laybutt DR, Preston AM, Akerfeldt MC, Kench JG, Busch AK, et al. (2007) Endoplasmic reticulum stress contributes to beta cell apoptosis in type 2 diabetes. Diabetologia 50: 752–763.
13. Bachar E, Ariav Y, Ketzinel-Gilad M, Cerasi E, Kaiser N, et al. (2009) Glucose amplifies fatty acid-induced endoplasmic reticulum stress in pancreatic beta-cells via activation of mTORC1. PLoS ONE 4: e4954.
14. Li D, Yin X, Zmuda EJ, Wolford CC, Dong X, et al. (2008) The repression of IRS2 gene by ATF3, a stress-inducible gene, contributes to pancreatic beta-cell apoptosis. Diabetes 57: 635–644.
15. Hai T, Hartman MG (2001) The molecular biology and nomenclature of the activating transcription factor/cAMP responsive element binding family of transcription factors: activating transcription factor proteins and homeostasis. Gene 273: 1–11.
16. Martinez SC, Tanabe K, Cras-Meneur C, Abumrad NA, Bernal-Mizrachi E, et al. (2008) Inhibition of Foxo1 protects pancreatic islet beta-cells against fatty acid and endoplasmic reticulum stress-induced apoptosis. Diabetes 57: 846–859.
17. Ishihara H, Asano T, Tsukuda K, Katagiri H, Inukai K, et al. (1993) Pancreatic beta cell line MIN6 exhibits characteristics of glucose metabolism and glucose-stimulated insulin secretion similar to those of normal islets. Diabetologia 36: 1139–1145.
18. Hohmeier HE, Mulder H, Chen G, Henkel-Rieger R, Prentki M, et al. (2000) Isolation of INS-1-derived cell lines with robust ATP-sensitive K+ channel-dependent and -independent glucose-stimulated insulin secretion. Diabetes 49: 424–430.
19. Girish V, Vijayalakshmi A (2004) Affordable image analysis using NIH Image/ImageJ. Indian J Cancer 41: 47.
20. Bernal-Mizrachi E, Fatrai S, Johnson JD, Ohsugi M, Otani K, et al. (2004) Defective insulin secretion and increased susceptibility to experimental diabetes are induced by reduced Akt activity in pancreatic islet beta cells. J Clin Invest 114: 928–936.
21. Finlay D, Patel S, Dickson LM, Shpiro N, Marquez R, et al. (2004) Glycogen synthase kinase-3 regulates IGFBP-1 gene transcription through the thymine-rich insulin response element. BMC Mol Biol 5: 15.
22. Srinivasan S, Bernal-Mizrachi E, Ohsugi M, Permutt MA (2002) Glucose promotes pancreatic islet beta-cell survival through a PI 3-kinase/Akt-signaling pathway. Am J Physiol Endocrinol Metab 283: E784–793.
23. White MF (2002) IRS proteins and the common path to diabetes. Am J Physiol Endocrinol Metab 283: E413–422.
24. Srinivasan S, Ohsugi M, Liu Z, Fatrai S, Bernal-Mizrachi E, et al. (2005) Endoplasmic reticulum stress-induced apoptosis is partly mediated by reduced insulin signaling through phosphatidylinositol 3-kinase/Akt and increased glycogen synthase kinase-3beta in mouse insulinoma cells. Diabetes 54: 968–975.
25. Hartman MG, Lu D, Kim ML, Kociba GJ, Shukri T, et al. (2004) Role for activating transcription factor 3 in stress-induced beta-cell apoptosis. Mol Cell Biol 24: 5721–5732.
26. Ramalho RM, Viana RJ, Low WC, Steer CJ, Rodrigues CM (2008) Bile acids and apoptosis modulation: an emerging role in experimental Alzheimer's disease. Trends Mol Med 14: 54–62.
27. Shimano H (2007) SREBP-1c and TFE3, energy transcription factors that regulate hepatic insulin signaling. J Mol Med 85: 437–444.
28. Goldstein JL, DeBose-Boyd RA, Brown MS (2006) Protein sensors for membrane sterols. Cell 124: 35–46.
29. Kakuma T, Lee Y, Higa M, Wang Z, Pan W, et al. (2000) Leptin, troglitazone, and the expression of sterol regulatory element binding proteins in liver and pancreatic islets. Proc Natl Acad Sci U S A 97: 8536–8541.
30. Takahashi A, Motomura K, Kato T, Yoshikawa T, Nakagawa Y, et al. (2005) Transgenic mice overexpressing nuclear SREBP-1c in pancreatic beta-cells. Diabetes 54: 492–499.
31. Wang H, Kouri G, Wollheim CB (2005) ER stress and SREBP-1 activation are implicated in beta-cell glucolipotoxicity. J Cell Sci 118: 3905–3915.
32. Tanabe K, Liu Z, Patel S, Doble BW, Li L, et al. (2008) Genetic deficiency of glycogen synthase kinase-3beta corrects diabetes in mouse models of insulin resistance. PLoS Biol 6: e37.
33. Cunha DA, Hekerman P, Ladriere L, Bazarra-Castro A, Ortis F, et al. (2008) Initiation and execution of lipotoxic ER stress in pancreatic beta-cells. J Cell Sci 121: 2308–2318.
34. Urano F, Wang X, Bertolotti A, Zhang Y, Chung P, et al. (2000) Coupling of stress in the ER to activation of JNK protein kinases by transmembrane protein kinase IRE1. Science 287: 664–666.
35. Kawamori D, Kaneto H, Nakatani Y, Matsuoka TA, Matsuhisa M, et al. (2006) The forkhead transcription factor Foxo1 bridges the JNK pathway and the transcription factor PDX-1 through its intracellular translocation. J Biol Chem 281: 1091–1098.
36. Lee JN, Ye J (2004) Proteolytic activation of sterol regulatory element-binding protein induced by cellular stress through depletion of Insig-1. J Biol Chem 279: 45257–45265.
37. Lu D, Chen J, Hai T (2007) The regulation of ATF3 gene expression by mitogen-activated protein kinases. Biochem J 401: 559–567.
38. Altomonte J, Richter A, Harbaran S, Suriawinata J, Nakae J, et al. (2003) Inhibition of Foxo1 function is associated with improved fasting glycemia in diabetic mice. Am J Physiol Endocrinol Metab 285: E718–728.
39. Accili D, Arden KC (2004) FoxOs at the crossroads of cellular metabolism, differentiation, and transformation. Cell 117: 421–426.
40. Susztak K, Ciccone E, McCue P, Sharma K, Bottinger EP (2005) Multiple metabolic hits converge on CD36 as novel mediator of tubular epithelial apoptosis in diabetic nephropathy. PLoS Med 2: e45.
41. Paolisso G, Tataranni PA, Foley JE, Bogardus C, Howard BV, et al. (1995) A high concentration of fasting plasma non-esterified fatty acids is a risk factor for the development of NIDDM. Diabetologia 38: 1213–1217.
42. El-Assaad W, Buteau J, Peyot ML, Nolan C, Roduit R, et al. (2003) Saturated fatty acids synergize with elevated glucose to cause pancreatic beta-cell death. Endocrinology 144: 4154–4163.
43. Prentki M, Joly E, El-Assaad W, Roduit R (2002) Malonyl-CoA signaling, lipid partitioning, and glucolipotoxicity: role in beta-cell adaptation and failure in the etiology of diabetes. Diabetes 51 Suppl 3: S405–413.

各論

# 膵β細胞死

太田康晴[1)]／谷澤幸生[2)]

〔SUMMARY〕 膵β細胞量は，複製，アポトーシス，新生のバランスによって決定されるが，2型糖尿病における膵β細胞量の減少はアポトーシスの増加によるとされている．しかし，実際にはアポトーシスの定量は困難であるため，残存膵β細胞量を解析することで，アポトーシスの定量を代用するというのが現状である．グルコース負荷後のインスリン反応が，空腹時のデータを元に算出するHOMA-βなどに比べて，より鋭敏に膵β細胞量を反映する指標であることが示されている．現時点では，*in vivo*で膵β細胞量を定量する技術は実用化されていないが，MRI，PETが，将来実用化が期待される侵襲のない，膵β細胞量イメージングの代表的な方法である．OPTは，3D画像によるイメージングの方法として期待が大きい．

〔臨床検査　54：1040-1047，2010〕

〔KEYWORDS〕 膵β細胞量，アポトーシス，イメージング

## 糖尿病の病態と膵β細胞量

糖尿病は，主にその成因により分類されている．1型糖尿病は，膵β細胞量の絶対的な減少によるもので，特に1A型では自己免疫学機序による膵β細胞の破壊が病態の主体である．2型糖尿病では，多くの場合，膵β細胞からのインスリン分泌の障害と肝臓や骨格筋などにおけるインスリン抵抗性の両者が認められる．2型糖尿病の病態形成において，インスリン分泌の障害とインスリン抵抗性のどちらが重要であるのかについては，長期間にわたる論争があった．2型糖尿病の発症初期には，高インスリン血症がしばしば認められることより，2型糖尿病では膵β細胞にprimaryな異常はないという考え方があった．しかし，ここ最近の研究成果より，2型糖尿病は，膵β細胞にもともと何らかの障害を有する場合に発症するという考え方が主流となってきている．

Butlerら[1)]は剖検膵組織の検討から，2型糖尿病患者において膵β細胞量が減少していることを報告した(図1)．この報告によれば，空腹時血糖がIGTの領域にある肥満患者の膵β細胞量は，正常血糖の肥満者に比べて少ないことがわかる．つまり，代償的肥大(過形成)を経て，何らかの要因で膵β細胞が減少に転じた個体，あるいは膵β細胞の代償的肥大(過形成)能力がもともと弱い個体において，血糖上昇が起こると考えられる．空腹時血糖が糖尿病領域まで達した個体では，さらに膵β細胞量は小さくなり，非肥満2型糖尿病患者においても膵β細胞量の減少は有意である．英国で行われたUKPDS(U.K. Prospective Diabetes Study)[2)]で，膵β細胞のインスリン分泌能が糖尿病発症の10～12年前から始まっていることが推察されたが，Butlerらの結果は，2型糖尿病発症時すでに膵β細胞の数(容量)の減少も起こっていることを示していると考えられる．

つまり，膵β細胞の容量(膵β細胞量)は，1型糖尿病のみならず，2型糖尿病の発症・進展においても重要な因子であり，インスリン抵抗性があっても，生体の需要に応じて，膵β細胞が自

1）山口大学大学院医学系研究科病態制御内科学・助教
2）同・教授

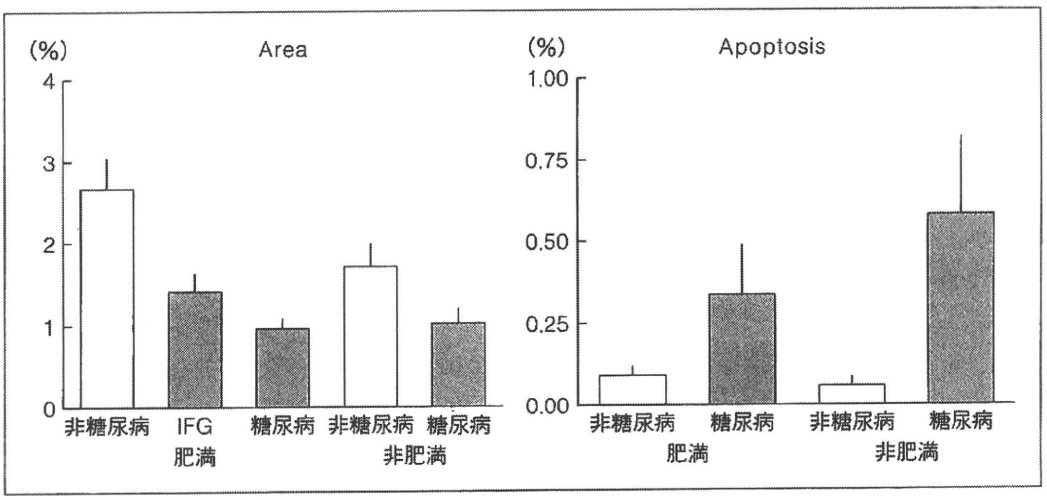


**図1　2型糖尿病における膵β細胞の容量(面積比，左)とアポトーシス(右)**

〔文献1)より引用〕

らその容量を増大させてインスリンを適切に分泌し続ける間は糖尿病を発症しない．しかし，インスリンの需要に対して見合うだけのインスリンが供給できなくなった状態，膵β細胞の容量を増大させることができなくなった状態で，糖尿病が発症することが推測される．

## 膵β細胞量と膵β細胞死

膵β細胞量の調節には，①膵β細胞自体の再生，②膵β細胞の大きさ，③膵β細胞の新生，④膵β細胞のアポトーシス，の4つの要素が密接に関連していると考えられている[3]．Butlerらの報告によると，再生と新生には，糖尿病群と非糖尿病群で有意差は認められなかったが，アポトーシスにおいてのみ有意差が認められたため(図1)，アポトーシスがヒトの膵β細胞量の調節には最も重要な因子であることが推察される．しかし，特殊な状況下でない限り，一時期にアポトーシスを起こしている膵β細胞の割合はラ氏島数当たり1%にも満たない．そのため，膵β細胞死(アポトーシス)を生体でリアルタイムに，特にヒトの生体で評価するのは極めて困難であり，現在もなお不可能であると言わざるをえない．

そう考えると，膵β細胞死というものは，残存膵β細胞量で代用して評価するしかないと考えられる．一方で，膵β細胞量を生体内で定量することに関しては，いくつかの優れた知見が得られてきている．そうした状況を踏まえ，膵β細胞死の検査を代用するものとして，(残存)膵β細胞量の定量を中心に概説したい．

## *In vivo* 検査による膵β細胞量の評価

### 1．動物モデル

膵β細胞死を病理所見以外で評価するのは現時点では不可能であり，その代用として残存膵β細胞量で評価することでさえ実際には容易なことではない．最も多い試みとしては，インスリン分泌能を評価することで，膵β細胞量を推測しようとすることである．

ミニブタを使った研究では，*in vivo* 検査と病理所見から得られた実際の膵β細胞量との関連を見出そうとしている．2003年には，ミニブタをストレプトゾトシン処理することで膵β細胞を死滅させ，インスリン分泌を評価すると，経静脈的グルコース負荷時の急性インスリン分泌応答(acute insulin response；AIR)とBCM(β cell mass)との間に良好な相関($r^2=0.6155$)が得られたことが報告された[4]．

### 2．HOMA-β(homeostasis model assessment β cell function)，AIR，C-ペプチドによる膵β細胞量の評価

1型糖尿病では，何らかの誘因によって膵β細胞容量が徐々に減少し，残存膵β細胞量が10%前後となったときに糖尿病を発症するとされている[5]．これと同じようなことが，2型糖尿病でも

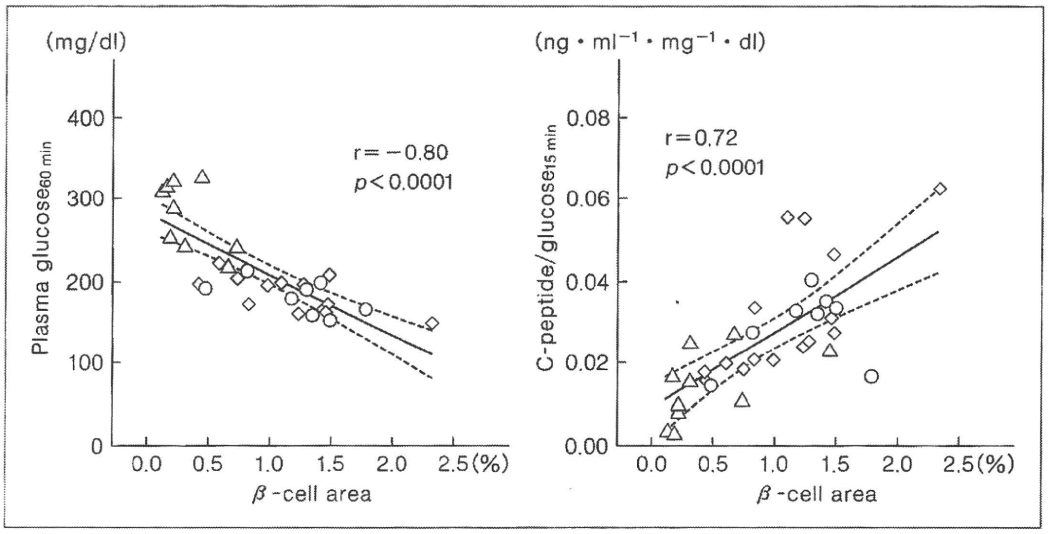


**図2　ヒトの摘出膵を用いた膵β細胞量とOGTT負荷後血糖値(30分，左)と負荷後C-peptide(15分，右)との相関**

○：NGT，◇：IGT，△：DM.

〔文献8)より引用〕

起こっていることが「ジョスリン糖尿病学」にも記されている．ここでは，UKPDSの患者データを基に，HOMA-βを算出して膵β細胞機能を推定するということが行われている．HOMA-βは“HOMA-β＝空腹時インスリン濃度(μU/ml)×360/空腹時血糖(mg/dl)－63”の計算式で算出される．

HOMA-βは，ADOPT(a diabetes outcome progression trial)studyにおいても，経時的に膵β細胞機能を評価するために用いられている[6]．しかしその一方で，HOMA-βは，AIRや血中プロインスリン濃度に比べて，膵β細胞機能障害を過小評価するものであることを示すデータもある[7]．HOMA-βは，負荷試験なしで算出できるというメリットをもっているが，やはりAIRに比べるとその評価は低いと考えられる．

また，ヒトの慢性膵炎や膵良性腫瘍の患者に対し，術前にOGTT(oral glucose tolerance test)などを行い，術後に摘出膵の組織を用いて，膵β細胞量(ここではエリア)とどの検査マーカーがよく相関するのかを調べた結果が報告された．その報告によると，負荷後のグルコース濃度や負荷後のC-ペプチド値は，膵β細胞量と非常に高い相関性を示すが(図2)，HOMA-βとは全くと言ってよいほど相関性が認められなかった[8]．この結果からも，少なくともある時間断面でのHOMA-βの絶対値は，残存膵β細胞量を評価する指標にはならない可能性が高いことがわかる．一連の解析の中で，膵β細胞量は空腹時のC-ペプチド/グルコースとも相関を示したため，空腹時であっても，血中C-ペプチドは膵β細胞量の指標となりうることが示唆された．

尿中C-ペプチド排泄量もインスリン分泌量を評価されるためによく用いられるため，膵β細胞量の指標としても有用ではないかと考えられる．しかし，C-ペプチドの尿排泄率には個人差が大きく，同一人ですら一定しないという問題もある．

空腹時にグルカゴン1 mgを静注し，静注前と6分後の血中C-ペプチドを測定するグルカゴン負荷試験も膵β細胞の機能・量の指標として有用であると考えられている．実際に日本人2型糖尿病患者にグルカゴン負荷試験を実施したところ，罹病期間が長期になるに従い負荷後C-ペプチド値が低下してくることが報告されている[9]．

## ● イメージングによる膵β細胞量の測定

### 1．膵ラ氏島の大きさとイメージング機器の開発

膵ラ氏島にはβ細胞以外の細胞も存在するため，厳密には膵ラ氏島の容量は膵β細胞量と同じではない．膵ラ氏島でさえ，その大きさは数十

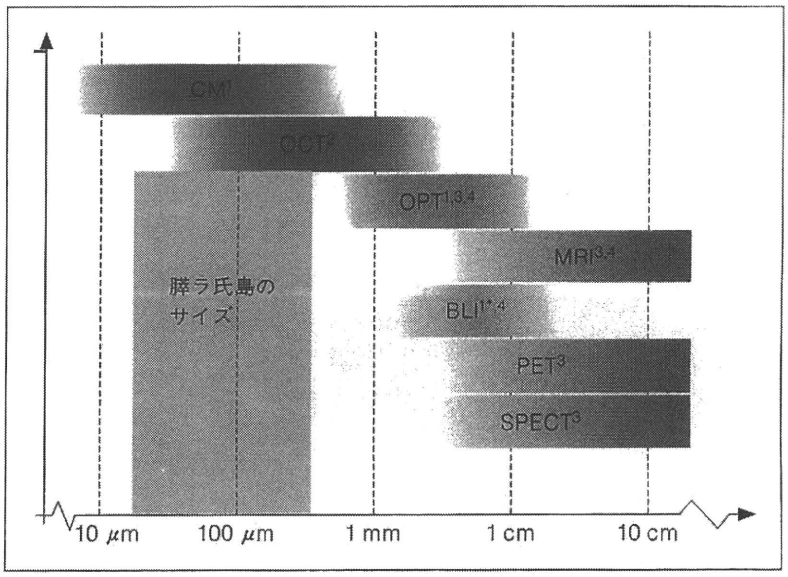


**図3　膵ラ氏島定量に使用される機器の空間分解能**
CM：confocal microscppy，OCT：optical coherence tomography，OPT：optical projection tomography，BLI：bioluminescent imaging，MRI：magnetic resonance imaging，PET：positron emission tomography，SPECT：single photon emission computed tomography.

〔文献10)より引用〕

～数百 μm ほどしかなく，膵 β 細胞量を膵ラ氏島量に置き換えて定量するとしても容易なことではない．

近年，科学の進歩に伴い，膵ラ氏島量の定量化に使用しうる機器も増えてきた(図3)[10]．OCTやOCMでは，膵ラ氏島量の定量可能なレベルまでその空間分解能は向上していると言える．しかしながら，これらは観察できる範囲が限定されており，OPTは摘出膵の標本を用いる必要がある．いずれにしてもヒトの膵ラ氏島量を生体のまま定量するのは，どちらを用いても現在のところ不可能である．BLI，MRI，PETにおいては，いずれも生体のままでの撮像が可能であるが，空間分解能は個々の膵ラ氏島を検知するレベルには至っていない．

### 2．confocal microscopy(共焦点顕微鏡)

光源としてレーザーが用いられるため“レーザー走査型共焦点顕微鏡”(共焦点顕微鏡)とも呼ばれている．共焦点顕微鏡では，焦点位置だけの情報がピンホールを通過して検出器に到達し，焦点位置以外の光はピンホールでカットされ，焦点のあった面だけの情報が得られるため，解像・コントラストが飛躍的に向上する．特に，深さ方向(Z方向)に分解能が生じ，光学的断層像を得ることができる[11]．空間分解能は，膵ラ氏島の大きさをはるかに上回るものである．しかし，非常に限られた深さ方向の解析しかできないため臓器全体の解析には不向きであること，また *in vivo* での観察ということになると，前眼部の観察など方法が限られていることより，今のところ膵ラ氏島量を *in vivo* で把握するということについては実用化されていない．

### 3．OCT(optical coherence tomography)

自然光に近い低コヒーレンス光(近赤外線の波長)を生体試料に照射して，その内部で反射した光波を高感度に検出する方法であり，OCTと呼ばれている．空間分解能は高く，膵ラ氏島を十分識別することができるレベルにある．膵管や血管にプローブを挿入することにより，理論的には *in vivo* での膵ラ氏島量の測定が可能になる．1番の問題は組織透過性が1～2 mmと非常に小さいことであり，膵ラ氏島量測定の実用化に向けてはこの問題の解決が必須である．

### 4．OCM(optical coherence microscopy)

最近，従来のOCMの弱点であった組織透過性とスキャン時間を大幅に改善することにより，

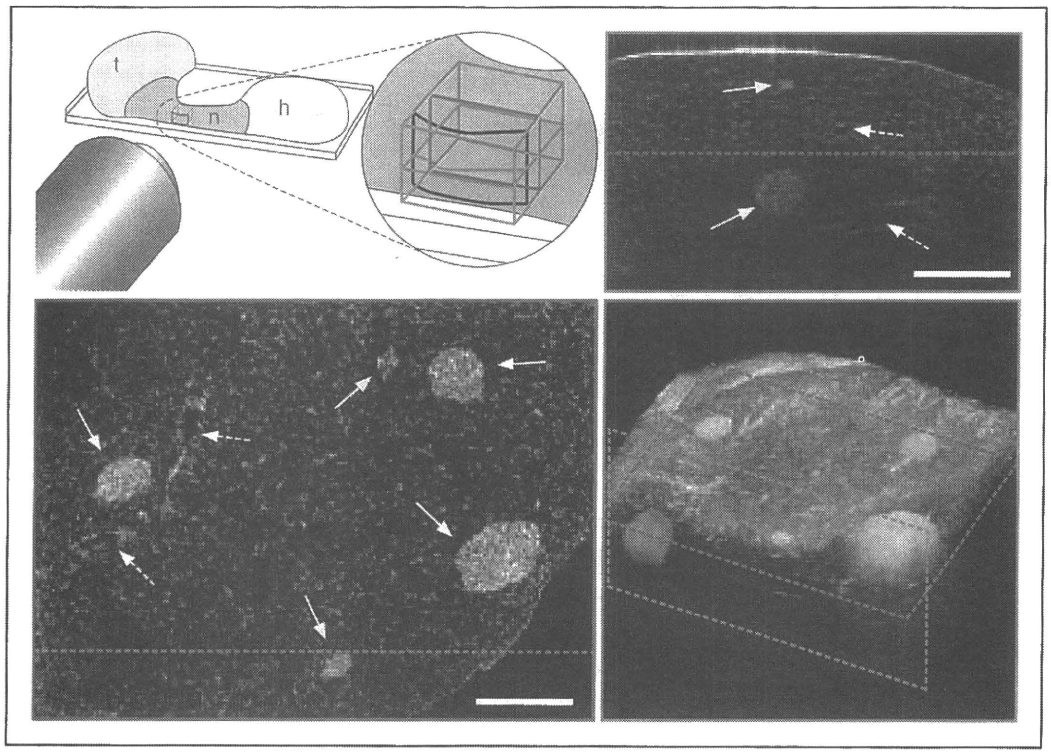


**図4　fx OCM(extended focus OCM)の測定原理**
まず緑色の面の画像を作製し(b)，それを赤色の面(c)と並行な方向に画像を重ねることにより，水色で囲まれたような3D画像(d)を得ることができる．実線矢印はラ氏島を，破線矢印は脈管を示している．

〔文献12)より引用〕

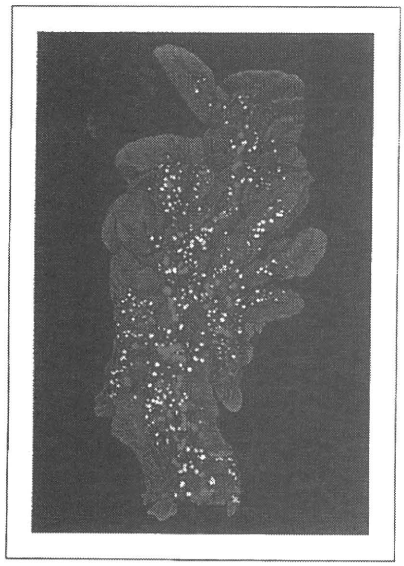

**図5　OPTによる膵β細胞の解析**
NOD(non obese diabetic)マウスから膵を摘出後，インスリン抗体の免疫染色を行っている．グレーは膵のアウトラインを示しており，赤，白，緑は膵ラ氏島を表すが，色によって膵ラ氏島の大きさが区別できる．

〔文献10)より改変〕

*ex vivo* のみならず *in vivo* でも膵全体にわたるラ氏島量を測定できるということが報告された[12]．3D画像を構築することにより，一個一個のラ氏島の容量を測ることができる(図4)．*in vivo* で測定する際には，膵臓を露出させる必要があるため，現時点ではヒトには応用できないが，今後，改良次第では臨床応用が可能になるかもしれない．

### 5．OPT(optical projection tomography：光投射型断層撮影技術)

CTスキャンの原理を可視光および紫外線に応用した技術を用いた3次元イメージングシステムである．OPTは1cm程度の小さなサンプルの高精度な3D解析を可能にしたと言える．この大きさは，共焦点顕微鏡では大きすぎ，MRIなどでは小さすぎるため，かつてはサンプルの凍結切片などを作成してから手作業で3次元画像を作っていた．空間分解能は5～50 μmであり，膵ラ氏島を十分に認識できるレベルにある(図5)[10]．

1型糖尿病のモデルマウスであるNOD(non obese diabetic)マウスの膵β細胞量が明らかに

減っていることをOPTで示したということも報告されている[13]．しかし現時点では，摘出膵に免疫染色などの処理を行う必要があり，ヒトの生体での臨床応用にはまだ課題が多い．

6．BLI(bioluminescent imaging)

ルシフェラーゼ遺伝子を発現している個体に発光基質を注射すると生体内で酸化反応(Luciferin-Luciferase反応)が開始され，その発光シグナルは非侵襲的に検出することが可能である．BLIではこの化学発光が利用されている．BLIは，もともと膵β細胞量を非侵襲的にモニタリングするために使われてきたという経緯があり，膵β細胞でルシフェラーゼを発現する遺伝子改変マウスを用いると，膵ラ氏島量を生体のまま光子量として測定できることが報告されている[14]．しかし，ヒトにおいて膵β細胞特異的にルシフェラーゼを発現させることは現在のところ困難である．

7．MRI(magnetic resonance imaging)

酸化鉄ナノ粒子で炭化デキストランコーティングした造影剤を用いて，MR画像での膵ラ氏島の可視化が試みられてきた．

CD8陽性のT細胞レセプターに特異的に結合するプローブを含む造影剤を用いることによって，NODマウスのラ氏島炎をMR画像でモニタリングできることが報告されている[15]．

Jirák ら[16]は，Resovist®という市販のMR造影剤の中で移植前の膵ラ氏島を培養した後，門脈内に注入し，膵ラ氏島移植を行っている．膵ラ氏島移植後の肝臓のMRIで膵ラ氏島が低信号イメージとして検出できることを報告している．この方法はヒトでも応用できるため，1型糖尿病の膵ラ氏島移植後の生着状況を確認する方法として期待されている．

8．PET(positron emission tomography)

内因性の残存膵ラ氏島を非侵襲的に映し出すことは不可能である．したがって実際には，膵β細胞特異的なプローブを利用して周辺とのコントラストを発生させ，PETによってそのシグナルを膵β細胞量として定量するアプローチが必要である．

プローブとしては，膵β細胞に特異的に発現している蛋白のリガンドや基質，そして特異的抗体などが候補となる．糖輸送担体であるGLUT2の基質である2-deoxy-glucoseやMannoheptulose[17]，スルホニルウレア受容体(SUR1)のリガンドであるSU薬[18]，ソマトスタチン受容体のリガンド[19]，小胞モノアミン輸送担体のリガンドであるDTBZ(dihydrotetrabenazine)[20]などがプローブとして有効であることが報告されている．

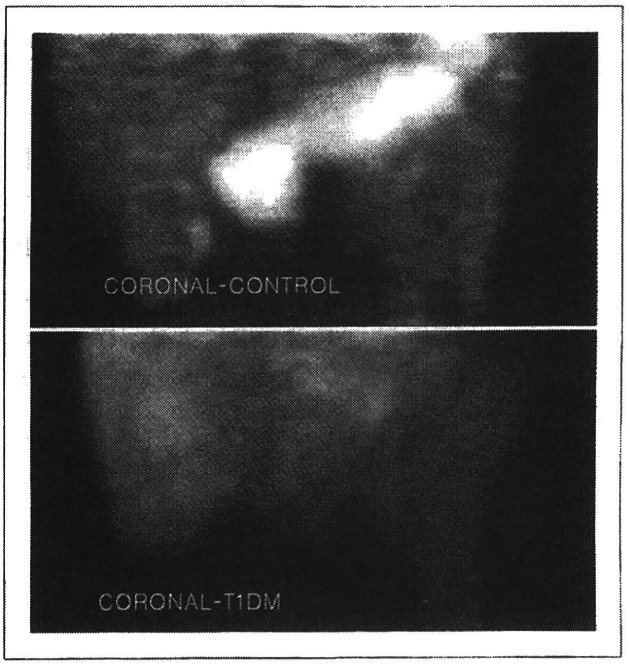


**図6　ヒトにおける[11C]-DTBZによる膵臓のイメージング**

1型糖尿病症例でのRI集積は正常者に比べて著明に減少している(矢印は膵臓を示す)．

〔文献21)より引用〕

VMAT2(vesicular monoamine transporter type2)は神経細胞の神経伝達物質顆粒に発現するトランスポーターで，膵β細胞の分泌顆粒にも発現している．膵β細胞のマーカーとしてのVMAT2ターゲッティング放射線標識リガンドの11C-DTBZを投与した後のPETで，1型糖尿病患者の膵臓への集積が正常人に比べて著明に低下していることが示されている(図6)[21]．

また，最近，RI標識したGLP-1受容体リガンドを用いることにより膵β細胞量を定量できることを，京都大学のグループが報告している[22]．

## おわりに

膵β細胞死をリアルタイムに評価するのは極めて困難で，残存膵β細胞量を評価することで代用するしかない．インクレチン関連薬は膵ラ氏島量を維持または増加させる可能性があることより，インクレチン関連薬の登場により，糖尿病の病態における膵β細胞死と残存膵β細胞量を評価することの重要性が一段と高まってきている．糖尿病の病態の理解とよりよい治療介入のために膵β細胞の量的変化を評価できる技術開発が求められる．

### 文　献


1) Butler AE, Janson J, Bonner-Weir S, et al : Beta-cell deficit and increased beta-cell apoptosis in humans with type 2 diabetes. Diabetes 52 : 102-110, 2003
2) U.K. prospective diabetes study 16. Overview of 6 years' therapy of type II diabetes : a progressive disease. U.K. Prospective Diabetes Study Group. Diabetes 44 : 1249-1258, 1995
3) Rhodes CG, Type 2 diabetes-a matter of beta-cell life and death? Science 307 : 380-384, 2005
4) Larsen MO, Rolin B, Wilken M, et al : Measurements of insulin secretory capacity and glucose tolerance to predict pancreatic beta-cell mass *in vivo* in the nicotinamide/streptozotocin Göttingen minipig, a model of moderate insulin deficiency and diabetes. Diabetes 52 : 118-123, 2003
5) Eisenbarth GS : Type I diabetes mellitus. A chronic autoimmune disease. N Engl J Med 314 : 1360-1368, 1986
6) Kahn SE, Haffner SM, Heise MA, et al : Glycemic durability of rosiglitazone, metformin, or glyburide monotherapy. N Engl J Med 355 : 2427-2443, 2006
7) Festa A, Williams K, Hanley AJ, et al : Beta-cell dysfunction in subjects with impaired glucose tolerance and early type 2 diabetes : comparison of surrogate markers with first-phase insulin secretion from an intravenous glucose tolerance test. Diabetes 57 : 1638-1644, 2008
8) Meier JJ, Menge BA, Breuer TG, et al : Functional assessment of pancreatic beta-cell area in humans. Diabetes 58 : 1595-1603, 2009
9) 藤本新平：グルカゴン負荷試験より検討したインスリン分泌不全の進展．糖尿診療マスター 7 : 231-234, 2009
10) Holmberg D, Ahlgren U : Imaging the pancreas : from *ex vivo* to non-invasive technology. Diabetologia 51 : 2148-2154, 2008
11) 阿部勝行：光学顕微鏡の現状．医療機器学 79 : 662-668, 2009
12) Villiger M, Goulley J, Friedrich M, et al : *In vivo* imaging of murine endocrine islets of Langerhans with extended-focus optical coherence microscopy. Diabetologia 52 : 1599-1607, 2009
13) Alanentalo T, Asayesh A, Morrison H, et al : Tomographic molecular imaging and 3D quantification within adult mouse organs. Nat Methods 4 : 31-33, 2007
14) Mol Imaging. Apr-Jun 5 : 65-75, 2006
Smith SJ, Zhang H, Clermont AO, et al : *In vivo* monitoring of pancreatic beta-cells in a transgenic mouse model. Mol Imaging 5 : 65-75, 2006
15) Turvey SE, Swart E, Denis MC, et al : Noninvasive imaging of pancreatic inflammation and its reversal in type 1 diabetes. J Clin Invest 115 : 2454-2461, 2005
16) Jirák D, Kríz J, Herynek V, et al : MRI of transplanted pancreatic islets. Magn Reson Med 52 : 1228-1233, 2004
17) Malaisse WJ : On the track to the beta-cell. Diabetologia 44 : 393-406, 2001
18) Sweet IR, Cook DL, Lernmark A, et al : Systematic screening of potential beta-cell imaging agents. Biochem Biophys Res Commun 314 : 976-983, 2004
19) Amartey JK, Shi Y, Al-Jammaz I, et al : Radioiodinated naphthylalanine derivatives targeting pancreatic beta cells in normal and nonobese diabetic mice. Exp Diabetes Res 371716, 2008
20) Souza F, Simpson N, Raffo A, et al : Longitudinal noninvasive PET-based beta cell mass estimates in a spontaneous diabetes rat model. J Clin Invest 116 : 1506-1513, 2006
21) Harris PE, Ferrara C, Barba P, et al : VMAT2 gene expression and function as it applies to imaging beta-cell mass. J Mol Med 86 : 5-16, 2008
22) Mukai E, Toyoda K, Kimura H, et al : GLP-1 receptor antagonist as a potential probe for pancreatic beta-cell imaging. Biochem Biophys Res Commun 389 : 523-526, 2009



### *Summary*

Monitoring of pancreatic beta-cell cell death

*Yasuharu Ohta*[1], *Yukio Tanizawa*[2]

Regulation of the pancreatic β-cell mass involves a balance of replication, apoptosis, and regeneration. The mechanism underlying decreased β-cell mass in type2 diabetes is increased apoptosis. However,

apoptosis is a difficult process to measure because the dead cells are rapidly degraded. Therefore, studying remaining beta cell mass replaces quantification of apoptosis. Acute insulin response after glucose load appears to better predict beta-cell mass than fasting measures, such as the HOMA-$\beta$. Imaging modalities such as MRI and PET could be used clinically in the near future as methodologies for non-invasive imaging of islet mass. OPT would be more suitable for monitoring islet mass and allow whole pancreas 3D spatial analysis.

〔Rinsho Kensa 54 : 1040-1047, 2010〕

1, 2) Division of Endocrinology, Metabolism, Hematological Science and Therapeutics, Department of Bio-Signal Analysis, Yamaguchi University Graduate School of Medicine, 1-1-1 Minamikogushi, Ube, Yamaguchi 755-8505, Japan

6

特集 糖尿病と遺伝子

# Wolfram症候群

松永仁恵[1)]，谷澤幸生[2)]
1)山口大学大学院 医学系研究科 病態制御内科学分野
2)山口大学大学院 医学系研究科 病態制御内科学分野 教授

Wolfram症候群は，1938年に，家族性の若年発症の糖尿病(diabetes mellitus)と視神経萎縮(optic atrophy)を合併する症候群として初めて報告された[1)]．その後，尿崩症(diabetes insipidus)や感音性難聴(deafness)を合併しやすいことが報告され，主要な4徴候(diabetes insipidus，diabetes mellitus，optic atrophy，deafness)の頭文字をとってDIDMOAD syndromeとも呼ばれている．1998年にWolfram症候群の原因遺伝子「WFS1遺伝子」が同定され，各国における有病率や臨床的特徴が徐々に明らかになってきている．ここでは，Wolfram症候群の臨床的特徴やWFS1遺伝子について，これまでの報告，最近の知見を踏まえて解説する．

## Wolfram症候群の診断

Wolfram症候群（WFS）は，常染色体性に劣性遺伝し，若年発症のインスリン依存性糖尿病と視神経萎縮を主徴とする．典型例では3～8歳で発症するインスリン分泌不全による糖尿病が初発症状となり，遅れて視神経萎縮，尿崩症，難聴など多彩な精神・神経症状をきたす．Wolfram症候群を診断するためのminimal criteriaは若年発症の糖尿病と視神経萎縮の合併であり，現在のところは糖尿病と視神経萎縮をきたす他の疾患を除外し，遺伝子診断を組み合わせて診断している．

## Wolfram症候群の臨床症状(図1)

英国での調査によると，典型例では平均年齢6歳（生後3週～16歳）で糖尿病が発症する．Wolfram症候群でみられる糖尿病の原因は，インスリン分泌の低下によるものである．患者の剖検においては膵β細胞の選択的消失が報告されている[3)]．多くの例でインスリン治療が必要になるが，糖尿病発症後数年にわたって経口薬で治療されている症例も少数存在し，そのなかにはインスリン分泌低下が比較的緩徐に進行し，完全なインスリン依存状態に至らない場合もある．視神経萎縮は平均年齢11歳（生後6週～19歳）で発症し，視力低下と色覚異常をきたす．視神経萎縮は進行性であり，ほぼすべての患者が全盲となる．次いで平均年齢14歳（生後3ヵ月～40歳）で73％の患者に中枢性尿崩症を合併する．また難聴は平均年齢16歳(5～39歳)で62％の患者に合併し，感音性難聴となる．その他に尿路異常が30歳代，精神神経症状が40歳代で発症する．精神神経症状は小脳性運動失調や脳幹失調，末梢性神経障害，てんかん発作，精神障害など，症状は多彩である．最近の報告[18)]では，精神神経症状の発症は以前の報告より早く，平均年齢15歳で発症すると報告されている．またMRI所見では，これまでに報告されていた大脳，小脳，脳幹の萎縮以外に，T2 FLAIR画像で視放線に一致した白質領域の高吸収域や白質脳症，脳回の皮質形成異常を認めている．

糖尿病，視神経萎縮以外の兆候を合併するかどうかは症

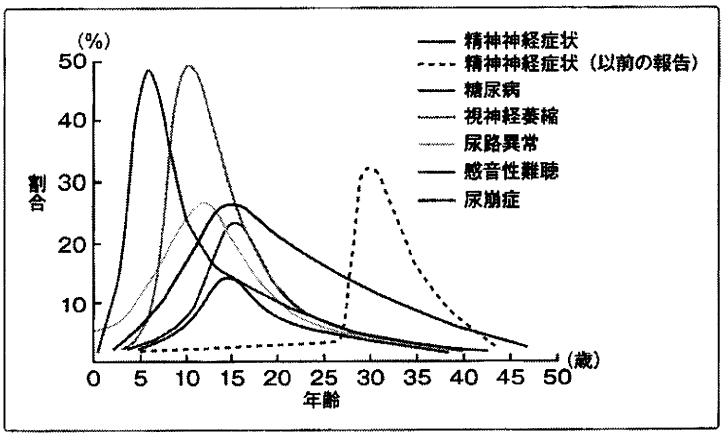


**図1 Wolfram症候群患者の臨床症状および各徴候の発症年齢（文献18）**
点線はBarretら[2]より報告された精神神経症状の発症年齢を示す．

例により異なるため，臨床像は多彩である．平均寿命は30歳（25歳～49歳）である．死因は30～40歳で発症する脳幹萎縮による呼吸不全や自殺によることが多い[2]．

## Wolfram症候群の治療

Wolfram症候群に対する根本的な治療は確立されていない．糖尿病に対してはインスリン療法を行い，尿崩症に対してはデスモプレシンの投与が行われる．その他，対症療法や支持療法を行い，患者QOLの向上を目指す．多彩な臨床症状を呈するため，包括的な診療体制を整備する必要がある．

## WFS1遺伝子の構造と機能

1998年にWolfram症候群の原因遺伝子としてWFS1遺伝子が同定された[4]．WFS1遺伝子は4番染色体短腕（4p16.1）に存在し，約33 kbpにわたる8つのエキソンにより構成される．第2エキソンに開始コドンがあり，第8エキソンの終わりに終止コドンが存在している（図2）．このうち第8エキソンが最も長く，遺伝子産物であるWFS1蛋白質（以下，WFS1）の68％をコードしている．現在までに多数のWolfram症候群患者で変異が同定されている（図2）．変異の大多数は最大エキソンである第8エキソンに存在し，変異の種類はミスセンス変異，ナンセンス変異，挿入・欠失変異など多岐にわたり，hot spotやfounder effect（創始者効果）を示唆する共通の変異は存在しない．

ヒトWFS1 cDNAから予想されるWFS1は890個のアミノ酸より構成され，分子量は100.3 kDaであった[4]．WFS1の構造が明らかとなった当時は，各種データベースの検索でも相同性を持つ蛋白は存在しなかったが，その後ショウジョウバエ，ハマダラカ，フグで相同性を持つ蛋白が同定されている．しかし，これらの機能はいずれも明らかでない．WFS1は小胞体に存在する9回膜貫通型の膜蛋白である[5,6]．加えて，膵臓ランゲルハンス氏島（以下，膵ラ氏島）β細胞ではインスリン分泌顆粒にも豊富に存在することが最近明らかになっている[15]．ノザン解析では，約3.7 kbの単一の転写産物が調べた臓器すべてに確認されたが，心臓・膵・胎盤での発現が多かった．組織内での発現には極性がみられ，膵ラ氏島に特異的に発現し，外分泌組織に発現はみられなかった．また中枢神経組織では，海馬（CA1），嗅結節，扁桃体および梨状皮質に強い発現が認められた．その他，弓状核や大脳皮質第2層にも発現が認められた[5]．

## Wolfram症候群の遺伝的多様性

Wolfram症候群の遺伝的多様性も報告されている．El-Shantiらは，ヨルダンの4家系において第2のWolfram症候群遺伝子*WFS2*が4番染色体長腕（4q22-24）に存在することを示した[7]．WFS2遺伝子変異によるWolfram症候群患者の臨床症状は従来報告されているWolfram症候